atmosphere

MDPI

Article

Assessment of Natural Radioactivity and Radon Exhalation in Peruvian Gold Mine Tailings to Produce a Geopolymer Cement

Rafael Liza [1,*], Patrizia Pereyra [1], Jose Rau [1], Maribel Guzman [1], Laszlo Sajo-Bohus [2,3] and Daniel Palacios [1]

[1] Pontificia Universidad Católica del Perú, Av. Universitaria 1801, Lima 15088, Peru
[2] Laboratorio de Física Nuclear, Universidad Simón Bolívar, Caracas 1080 A, Venezuela
[3] Alba Regia Technical Faculty, Óbuda University, 8000 Szekesfehervar, Hungary
* Correspondence: raliza@pucp.edu.pe

Abstract: Mining generates significant amounts of waste that can represent a source of contamination for areas close to the extraction area, generating a negative impact both on the environment and the health of people. This study aims to evaluate the radiological risk derived from exposure to natural radionuclides contained in tailings from Peruvian gold mines and to establish whether the tailings can be used as raw materials in building materials. The mine tailings come from a mining project in the northern highlands of Peru. Radon exhalation was measured using Rad7 in a closed chamber and activity concentration of ^{226}Ra, ^{232}Th, and ^{40}K radioisotopes by gamma spectrometry using NaI 3″ × 3″ detector. Maximum activity concentrations measured for ^{226}Ra and ^{232}Th were 15.38 Bq kg^{-1} and 11.9 Bq kg^{-1}, respectively; meanwhile, activity concentration for ^{40}K ranged from 182.7 Bq kg^{-1} to 770.8 Bq kg^{-1}. All activity concentrations were below the worldwide average except for ^{40}K. The radon exhalation rate varied from 2.8 to 7.2 mBq kg^{-1} h^{-1}. The gamma index (I_γ), and radiological parameters, including the Radium equivalent activity (Ra_{eq}), and the external hazard index (H_{ex}), being below the recommended levels by UNSCEAR, ensure the safe use of these mines tailing to produce a geopolymer cement.

Keywords: gold mine tailings; radon exhalation; activity concentration; radiological hazard; gamma spectroscopy

check for updates

Citation: Liza, R.; Pereyra, P.; Rau, J.; Guzman, M.; Sajo-Bohus, L.; Palacios, D. Assessment of Natural Radioactivity and Radon Exhalation in Peruvian Gold Mine Tailings to Produce a Geopolymer Cement. *Atmosphere* **2023**, *14*, 588. https://doi.org/10.3390/atmos14030588

Academic Editors: Federica Leonardi, Giorgia Cinelli and Daniel Rabago

Received: 8 February 2023
Revised: 7 March 2023
Accepted: 15 March 2023
Published: 19 March 2023

Copyright: © 2023 by the authors. Licensee MDPI, Basel, Switzerland. This article is an open access article distributed under the terms and conditions of the Creative Commons Attribution (CC BY) license (https://creativecommons.org/licenses/by/4.0/).

1. Introduction

Mining is an essential component in the progress of human civilization and has a significant impact on the economies of numerous countries worldwide. Geopolymer cement is a sustainable alternative to traditional Portland cement, made by using industrial waste materials such as mine tailings [1]. In recent years, the use of geopolymer cement in infrastructure projects has been growing due to its low carbon footprint and potential for reducing the environmental impact of construction [2,3]. In Peru, where mining is a significant industry, the use of mine tailings in geopolymer cement production presents an opportunity to create a more sustainable building material. However, the use of such materials as an additive may raise concerns about the possibility to have higher than recommended concentrations of radionuclides in the final product [4]. Studies carried out at gold mines across the world have indicated that the average concentration of primary radionuclides in gold mine tailings is in some cases comparably higher than the worldwide average [5,6]. On the other hand, studies have shown that copper [7–9], gold [10–12], and iron [13–16] mine tailings can be used as a partial substitute for cement in concrete construction, improving its compressive strength and reducing heavy metal pollution in the environment [17]. Recently, scientists have investigated the utilization of mine tailings in the construction industry as a substitute for cement in concrete, with varying degrees of substitution, or as an ingredient in the production of cement [18–20]. Peru is one of the leading producers of metals in the world, and its mining industry contributes significantly

to the economy of the country. However, mining also generates large amounts of mine tailings, which are a byproduct of mineral extraction and can be harmful to the environment and the health of people if not managed properly.

Mine tailings are solid waste produced during mineral processing and may contain toxic substances such as heavy metals and radioactive substances [21]. To mitigate the effects of mine tailings, various techniques have been developed, such as the proper and safe handling of mine tailings, the revegetation and rehabilitation of areas affected by mining activities, and the reuse of mine tailings in other sectors, such as construction [22,23]. The use of mine tailings in construction is one of the main ways to recycle these wastes and reduce their environmental impact [24]. This approach is aligned with the principles of the circular economy, which is based on designing more sustainable systems that maximize the reuse and recycling of resources, reduce waste generation, and minimize the environmental impact of human activities [25]. Certain metal ores, and some copper and gold deposits, have been found to have associated naturally occurring radioactive materials (NORM). Although the concentration of NORM is generally low in most natural materials, any activity involving the extraction and processing of materials from the earth can result in an increased NORM concentration. Like all building materials containing NORM, cement is also a source of ^{222}Rn inside homes. Thus, from a radiological protection viewpoint, it is essential to know the contribution of building materials to the levels of radon concentration in indoor air since radon is considered a carcinogen by the World Health Organization [26]. Radon emanation is the fraction of radon atoms produced in the grain of material that can escape to interstitial space depending on its location within the grain at the time of ^{226}Ra disintegration. Those atoms move through the pores of the material until it reaches the surface and is released into the indoor environment; this process is commonly referred to as radon exhalation [27]. The exhalation of radon from building materials is influenced by the concentration and distribution of ^{226}Ra in the material, as well as physical properties such as porosity, particle size, water content, and permeability [28,29]. Several external factors can also affect the radon exhalation rate, including atmospheric pressure, humidity, and temperature [30]. The measurement of the radon exhalation rate from these materials can help to select suitable building materials from the radiological point of view. On the other hand, if a dwelling has already been constructed, the radon exhalation from building materials can be measured to identify appropriate mitigation strategies such as ensuring adequate ventilation and conducting air testing. Common building materials generally have a minimal impact on indoor radon levels; however, some of them may have elevated levels of ^{226}Ra and can be significant sources [31–33]. In the case of new building materials made from mining tailings, it is important to conduct a radiological study to determine whether they are suitable for use as building materials.

This study aims to provide data on the concentration of natural radionuclides and radon exhalation to establish if selected gold–copper Peruvian mine tailings can be convenient to be used in the production of geopolymer cement. The materials and methods used included the collection and preparation of the samples, radon exhalation rate measurement, and gamma-spectrometric analysis. The radon mass exhalation rate and activity concentrations of ^{226}Ra, ^{232}Th, and ^{40}K were determined for mining tailings samples. Radiological parameters such as the radium equivalent (Ra_{eq}), gamma index (I_γ), alpha index (I_α), and external hazard (H_{ex}) were evaluated to assess the radiation risk associated with the mine tailings. The results of this study will contribute to the understanding of the potential environmental and health impacts of using mine tailings in geopolymer cement production and provide important information for stakeholders in the construction industry.

2. Materials and Methods

2.1. Sample Collection and Preparation

A total of 5 mine tailings samples from a gold mine were collected and analyzed. The mining company provided tailings samples selected for their chemical and geomechanical properties, to be assessed for use in a brick production feasibility project. These samples

were representative of the entire volume of tailings produced during the exploitation, based on previous studies conducted in brick manufacturing. The location of the mine is indicated on the map in Figure 1.

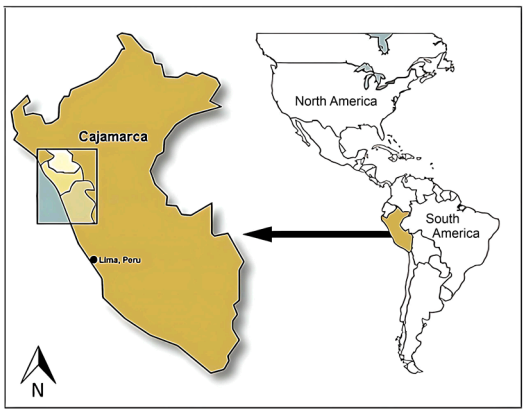

Figure 1. Gold mine location map in the northern highlands of Peru.

In a mining operation, it is necessary that the mining tailings contain a certain amount of water to form a pulp, which allows them to be transported. Once the tailings samples have been obtained, it is necessary to extract the excess water to carry out the brick manufacturing processes. Approximately half a ton of tailings was received, with an approximate solid content of 25%. Then, for the drying process, the pulp was sedimented by gravity to separate the supernatant water from the fine tailings. The liquid portion was discarded due to its low solid content. The solid portion was directly separated into large trays with an approximate weight of 4 kg for subsequent drying in a furnace at a temperature of around 50 °C [34]. The granulometric analysis of each sample allowed us to determine the D80 (mesh size of the opening of the sieve through which 80% of the solid that is being sieved passes). D80 values were 50.10 mm; 135.78 mm; 134.25 mm; 125.27 mm; and 134.92 mm for each sample, respectively [35].

Crystal phases were analyzed using X-ray diffraction (XRD). XRD analysis was performed using a Bruker D8 Discover model with a copper anode ($Cu_{K\alpha}$ = 0.15418 nm), a DC current of 40 mA, and an acceleration voltage of 40 kV, with a Lynxeye detector with energy selectivity. The analysis was conducted over a range of angles (2θ) from 5° to 80° in 0.02° steps. The reference intensity ratio (RIR) method was used to calculate the composition of the crystal phases and the amorphous portion.

Compositional analysis was conducted using X-ray fluorescence (XRF). The X-ray fluorescence analysis was conducted using the wavelength-dispersive X-ray spectrometer (WDXRF) Bruker S8 TIGER model, with a rhodium (Rh) anode, a DC current of 170 mA, and an acceleration voltage of 60 kV, with collimators with an aperture angle of 0.23° and 0.46°, in addition to the following analyzers crystals: PET, LIF (200), LIF (220), and XS-55, and two types of detectors: scintillation counter and flow proportional. The oxide evaluation model was employed, and the measurement time was 8 min for each sample. The fused bead method was used for sample preparation.

2.2. Gamma Spectrometry Analysis

Approximately 1000 g of the samples was placed in airtight containers (85.4 mm and 138 mm for internal diameter and filling height, respectively) and kept in the laboratory for 30 days to achieve secular equilibrium between ^{226}Ra, ^{222}Rn, and their short-lived progeny. The tightness of the cylindrical containers was ensured by covering the O-ring surface cap with high-vacuum grease. A leakage test was conducted using the AlphaGuard instrument operating in diffusion mode as a continuous radon monitor within an accumulation chamber made of methacrylate.

Gamma spectra were acquired for 86,400 s using an 3″ × 3″ NaI spectrometer. The MAESTRO®-32 (ORTEC, USA) MCA Emulation software (version 7.01) was used for peak identification, the setting of regions of interest (ROI), and the determination of net peak areas. Reference material IAEA-412 was placed on a tightly sealed petri plate and used for efficiency calibration. The extended relative method of activity determination (ERMAD) was used for quantification as the samples differed in geometry, composition, and density from the reference material [36]. The efficiency transfer factor required by ERMAD was estimated using the ETNA software (Laboratoire National Henri Becquerel, France, version 5.5) [37]. All of the samples were carefully placed into high-density cylindrical plastic containers, filling them completely.

For a 95% confidence level of peak detection, the minimum detectable activity (MDA) concentration in units of Bq kg^{-1} was calculated by [38]:

$$MDA = \frac{2.71 + 3.29\sqrt{2B_R \times t_C \times FWHM \times F/ECAL}}{\varepsilon \times P_\gamma \times t_C} \quad (1)$$

where B_R is the total background count rate; t_C is the live time of the count; $FWHM$ ($\leq$8.5% for ^{137}Cs) is the width of the spectrum curve, which is measured between two points (in energy units); F is the factor necessary for the desired coverage; $ECAL$ is the energy calibration factor to convert $FWHM$ into channels; ε is the efficiency of the detector at the energy of the measured gamma-ray; and P_γ is the gamma-ray emission probability.

2.3. Radon Exhalation Rate Measurement

For granular materials, the exhalation surface area is difficult to calculate accurately because it strongly depends on particle size according to Tuccimei et al. [39]. Therefore, in these cases, it is common to express the radon exhalation rate in terms of mass [40,41]. The radon mass exhalation rate was determined using a RAD7 instrument (Durridge Company Inc., Bedford, MA, USA) by the closed chamber method. A stainless-steel accumulation chamber with a cylindrical design was built for the purpose of exhalation measurements. The tightness test for the stainless-steel accumulation chamber was carried out by placing a sample of uranium ore inside this chamber and measuring the growth of the radon concentration in a closed loop using the RAD7 instrument. Leakage and back-diffusion have a significant impact on the accumulation chamber. However, if the measurement of radon exhalation is carried out over a short period (less than 24 h), it is possible to ignore these effects as other authors have considered [42,43]. The stainless-steel accumulation chamber was connected to the RAD7 instrument, creating a closed circuit as shown in Figure 2.

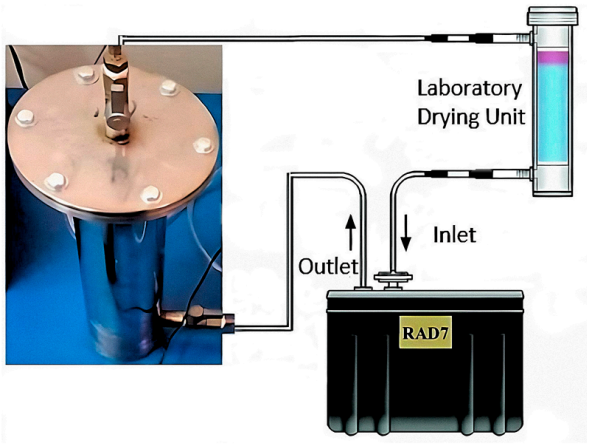

Figure 2. Experimental setup to assess ^{222}Rn exhalation rates from mine tailings samples using the Rad7.

The radon concentration $C(t)$ within the cylindrical stainless steel accumulation chamber can be described by the radon mass transfer equation as presented by [44]:

$$\frac{dC(t)}{dt} = \frac{E(t)S}{V_C} - \lambda_{R_n}C - \lambda_L C - \lambda_{BD}C \quad (2)$$

The solution can be written as:

$$C(t) = C_s + (C_0 - C_S)\mathrm{e}^{-\lambda_{eff}t} \quad (3)$$

where C_s represents the equilibrium radon concentration, C_0 is the initial radon concentration, $E(t)$ is the radon exhalation rate, S is the exhalation area, V_C is the free volume of the closed chamber including the RAD7 measuring system, and the effective decay constant is $\lambda_{eff} = \lambda_{Rn} + \lambda_{BD} + \lambda_L$. The terms λ_{BD}, λ_L, and λ_{Rn} represent the back-diffusion, the radon leak rate, and decay constant of radon, respectively. The accumulation of radon within the closed chamber is characterized by a linear increase in radon concentration over the first 24 h [45,46]. Then, the radon mass exhalation rate E (Bq kg^{-1} h^{-1}), considering λ_{BD} and λ_L, which are negligible for a short sampling period, can be obtained by [39]:

$$E = (m + \lambda_{Rn}C_0)\frac{V_C}{M} \quad (4)$$

where m (Bq m^{-3} h^{-1}) is the initial slope of radon growth in the accumulation chamber in the first 24 h, and M is the mass of the sample.

2.4. Evaluation of Activity Indexes and Radiological Hazard Parameters

The presence of natural radioactivity in building materials is commonly assessed through the evaluation of natural radionuclides ^{40}K, ^{232}Th, and ^{226}Ra. The radiological assessment of the studied mine tailings can be considered based on the indexes proposed for building materials as they will make up a significant proportion of their composition. However, the distribution of these radionuclides in the building materials being studied is not uniform.

2.4.1. Gamma Index (I_γ)

The Gamma index quantifies the effect of three radioactive isotopes ^{226}Ra, ^{232}Th, and ^{40}K (Bq kg^{-1}) present in building materials and is calculated using Equation (5) given by the European Commission [47]:

$$I_\gamma = \frac{C_{226_{\mathrm{Ra}}}}{300} + \frac{C_{232_{\mathrm{Th}}}}{200} + \frac{C_{40_{\mathrm{K}}}}{3000} \quad (5)$$

Building materials with a gamma index ≥ 1 possess the potential to result in annual effective doses surpassing 1 mSv. On the other hand, the value of the gamma index < 1 indicates the safe use of the analyzed material [47].

2.4.2. Alpha Index (I_α)

The alpha index is a term used to describe an excess of alpha radiation that may be present in a room due to the presence of the radon exhaled from building materials [48,49]:

$$I_\alpha = \frac{C_{226_{\mathrm{Ra}}}}{300} \leq 1 \quad (6)$$

The activity concentration of ^{226}Ra must not exceed 300 Bq kg^{-1}, to prevent exposure to indoor radon concentrations greater than 300 Bq m^{-3}, which is recommended by the EU and ICRP as the action level for indoor radon exposure in dwellings [48,50].

2.4.3. External Hazard Index (H_{ex})

This index assumes that the walls are thick, without windows or doors [51]. The external hazard index, designated as H_{ex}, calculates the expected radiation dose that results from the emission of γ-rays from building materials. For the radiation risk to be considered low, the H_{ex} value must be less than 1.

$$H_{ex} = \frac{C_{226_{Ra}}}{370} + \frac{C_{232_{Th}}}{259} + \frac{C_{40_K}}{4810} \quad (7)$$

2.4.4. Radium Equivalent Activity (Ra_{eq})

The radium equivalent activity index (Ra_{eq}) was developed as a means of representing the activity concentrations of ^{40}K, ^{232}Th, and ^{226}Ra as a single quantity, taking into consideration the associated radiation hazards. Furthermore, Ra_{eq} takes into consideration that the concentration activity of these radionuclides in building materials is not uniformly distributed and therefore does not emit an equal dose of radiation. Ra_{eq} is calculated using the following equation [51]:

$$Ra_{eq} = C_{226_{Ra}} + 1.43C_{232_{Th}} + 0.077C_{40_K} \quad (8)$$

The maximum permissible dose rate for any building material is 1 mSv y^{-1}, which is equivalent to 370 Bq kg^{-1} of Ra_{eq} [52].

3. Results and Discussion

3.1. Granulometric and Mineralogical Analysis

Grinding processes were used to extract the maximum amount of mineral, varying the grain size. Table 1 provides a detailed range of grain sizes for each tailing sample.

Table 1. Range of grain size in each mining tailing sample.

Samples	Grain Size (μm)
REL-1	(10–50)
REL-2	(78–135)
REL-3	(25–134)
REL-4	(27–125)
REL-5	(134–192)

X-ray diffraction analysis has been performed to determine the mineralogical composition of the mine tailing samples. Table 2 shows the concentration of crystal phases in the samples.

Table 2. Concentration (%) of observed crystal phases in the mining tailings samples analyzed by XRD.

Samples	REL-1	REL-2	REL-3	REL-4	REL-5
Quartz	74.5	79.4	21.5	29.6	81.0
Pyrite	8.0	2.0	16.3	14.9	2.7
Muscovite	0.9	1.5	11.2	11.6	1.5
Kaolinite	0.8	1.1	9.9	9.2	1.0
Others	15.8	16.0	41.1	34.7	13.8

3.2. Assesment of Radon Leakage from the Stainless-Steel Accumulation Chamber

To assess the radon leakage from the stainless-steel accumulation chamber, the concentration of ^{222}Rn was monitored over a 15-day period with data collected every 30 min. Considering that the initial radon concentration in the chamber, C0, is nearly zero at the beginning of the accumulation process or assuming that the initial radon concentration

inside the chamber is significantly smaller than the saturation [53], Equation (3) can be simplified as:

$$C(t) = C_s\left(1 - e^{-\lambda_{eff} \cdot t}\right) \quad (9)$$

The dataset was fitted using the exponential function in the form of Equation (9). The best fit for the growth of radon concentration, which estimates a concentration equilibrium value of 2957 Bq m^{-3}, is represented by the red line in Figure 3. A value of (0.0077 ± 0.0001) h^{-1} was obtained for the effective decay constant, which is very closed to radon decay constant $\lambda_{Rn} = 0.0076\ h^{-1}$. Thus, the radon concentration leakage can be considered negligible from the stainless-steel accumulation chamber since $\lambda_{eff} = \lambda_{Rn}$ [54].

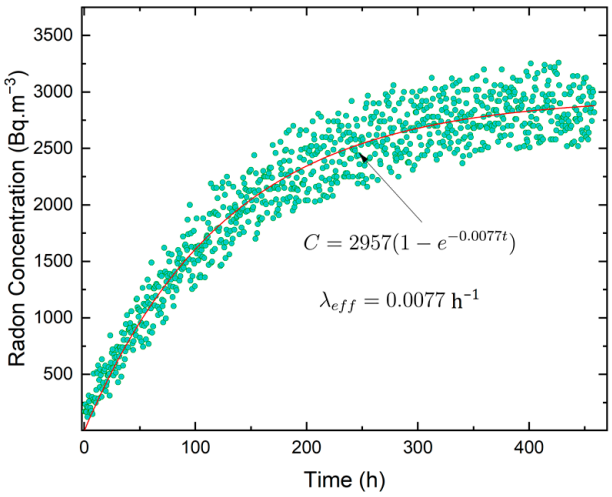

Figure 3. Experimental ^{222}Rn concentration growth and exponential fit of measured radon activity concentration inside the accumulation chamber.

3.3. Activity Concentrations of ^{226}Ra, ^{232}Th, and ^{40}K

Table 3 shows the activity concentrations for ^{226}Ra, ^{232}Th, and ^{40}K in Bq kg^{-1}. The activity ^{226}Ra was determined from 1760 keV peak from ^{214}Bi, the activity of ^{232}Th was determined from 2614 keV peak from ^{208}Tl, and the activity of ^{40}K was determined from 1460 keV peak. The MDA was 6.6 Bq kg^{-1} for ^{226}Ra, 6.2 Bq kg^{-1} for ^{232}Th, and 32 Bq kg^{-1} for ^{40}K. The variation in the activity concentrations of ^{226}Ra was found in the range from BDL to 15.4 Bq kg^{-1} with a mean value of 11.5 Bq kg^{-1}. ^{232}Th varied in the range from BDL to 9.0 Bq kg^{-1} with a mean value of 8.77 Bq kg^{-1}. ^{40}K ranged from 182.7 Bq kg^{-1} to 770.8Bq kg^{-1}, with a mean value of 479.1 Bq kg^{-1}. The average activity levels of ^{226}Ra, ^{232}Th, and ^{40}K in building materials worldwide are 35 Bq kg^{-1}, 30 Bq kg^{-1}, and 400 Bq kg^{-1}, respectively [55]. REL-4 and REL-5 have values higher than the global average for ^{40}K. In the case of the other radionuclides, all values are below worldwide levels. The contents of ^{226}Ra, ^{232}Th, and ^{40}K in REL-1 compared to those in other samples are of interest because of its smaller grain size (10–50 µm). The very low radium content in REL-1 and REL-2 could be explained by the higher proportion of quartz in their composition, which is 74.5% and 79.4%, respectively, as indicated in Table 2. REL-1 and REL-2 were simultaneously extracted from the same mine zone and subjected to different flotation processes; there is no significant difference in the ^{226}Ra and ^{232}Th content. Meanwhile, REL-1 and REL-2 were simultaneously extracted from a different zone of REL-3 and REL-4. The last two samples had the lowest proportion of quartz with 21.5% and 29.6%, respectively. These results show that the radionuclide contents are higher than in tailings 1 and 2, indicating heterogeneity in the concentration of the radionuclides depending on the extraction area. Finally, REL-5 has the highest amount of quartz, which could indicate that it has the lowest amount of natural radionuclides. However, as shown in Table 3, it has values comparable to REL-3 and REL-4 tailings. One possible explanation is that REL-5

was subjected to a grinding process that produced larger grain sizes, which increases the effective surface area for interaction with the chemical agents used in the flotation process, resulting in less impact on the concentration of natural radionuclides. At the same time, the flotation liquid has a significant potassium content, which could explain the higher levels of this element in samples REL-4 and REL-5. However, it is important to consider that the concentration of different chemical agents in the flotation liquid is not homogeneous, as dosing varies depending on the mineralogy, which is notably variable in a mine.

Table 3. Activity concentrations of ^{226}Ra, ^{232}Th, and ^{40}K (Bq kg^{-1}) in mining tailing samples.

Samples	Activity Concentrations in Bq kg^{-1}		
	C_{K40} (Bq kg^{-1})	C_{Ra226} (Bq kg^{-1})	C_{Th232} (Bq kg^{-1})
REL-1	183 ± 9	BDL	BDL
REL-2	229 ± 11	BDL	BDL
REL-3	461 ± 22	9.1 ± 1.4	5.5 ± 2.2
REL-4	771 ± 37	15.4 ± 2.4	8.9 ± 3.6
REL-5	752 ± 36	9.9 ± 0.5	11.9 ± 1.2

BDL: Below detection limit.

3.4. Radon Mass Exhalation Rate

Table 4 summarizes the radon mass exhalation rate for all samples and the slope of the fitted line, denoted as "m" (radon concentration versus time). The radon mass exhalation rate (ER) varies from (2.80 ± 0.34) mBq kg^{-1} h^{-1} to (7.20 ± 0.65) mBq kg^{-1} h^{-1} with an average value ± 1σ of (5.32 ± 1.73) mBq kg^{-1} h^{-1}. The five mine tailing samples of different grain sizes and calculations show different exhalation rates. Percentagewise, the difference between the radon exhalation rate of the sample with the lowest exhalation, REL-2, and the sample with the highest exhalation, REL-4, is 88%. The slope values are small due to the low radon exhalation rate, which in turn is conditioned by the poor ^{226}Ra content in samples. Sample REL-4 has a higher content of ^{226}Ra, possibly due to the lower quartz content and the possibility that the other minerals that make up this tailing may host a higher content of radium. In general, the values of radon mass exhalation rates from the mine tailing samples analyzed are relatively low, as indicated by these results.

Table 4. Slope and radon mass exhalation rate in mining tailing samples.

Samples	m + Δm [Bq m^{-3} h^{-1}]	ER + ΔER [mBq kg^{-1} h^{-1}]
REL-1	0.97 ± 0.07	4.40 ± 0.39
REL-2	0.98 ± 0.07	2.80 ± 0.34
REL-3	1.02 ± 0.07	5.90 ± 0.53
REL-4	1.11 ± 0.08	7.20 ± 0.65
REL-5	1.04 ± 0.07	6.30 ± 0.55

3.5. Activity Indexes and Radiological Hazard Parameters

Mean values of Gamma and Alpha indexes (I_γ, I_α), radium equivalent Ra_{eq}, and external hazard H_{ex} parameters are represented in Table 5. The Gamma Index I_γ in all samples was ≤0.5, corresponding to the exemption dose criterion of 0.3 mSv y^{-1}, so this material can be considered exempt and can be used as secondary raw material to produce cements without restrictions [47]. Similarly, all estimated alpha indexes I_α for the analyzed mine tailing samples fell within the range of 0.02 to 0.08, with an average of 0.03. These values were also within the recommended level of $I_\alpha < 1$, which corresponds to indoor radon concentration of less than 300 Bq·m^{-3}. Radium equivalent activity (Ra_{eq}) in mine tailing samples were (52.64 ± 32.27) Bq kg^{-1}, and the external hazard H_{ex} was 0.14 ± 0.09. The external hazard index H_{ex} is below one and falls below the safe recommended level. The radium equivalent Ra_{eq} values of the cement samples are lower than the recommended

level of 370 Bq m^{-3} [47,55]. As can be evidenced from Equations (5) and (7) if I_γ is less than 1, H_{ex} is also expected to be less than 1 because one equation is derived from the other. Therefore, H_{ex} is not necessary to be calculated if previously known that $I_\gamma < 1$.

Table 5. Average values of activity indexes and radiological hazard parameters.

Sample	I_γ	I_α	H_{ex}	Ra_{eq}
REL-1	0.08	0.02	0.05	19.93
REL-2	0.10	0.02	0.06	23.52
REL-3	0.21	0.05	0.14	52.42
REL-4	0.35	0.08	0.24	87.48
REL-5	0.34	0.05	0.23	84.85

4. Conclusions

The levels of ^{226}Ra, ^{232}Th was found significantly below the maximum allowed levels. Only in the case of ^{40}K, levels were slightly above the global average. The radon mass exhalation rate values were consistent with the levels of ^{226}Ra measured through gamma spectrometry. In general, the radon exhalation rate from the mine tailing samples is below the global average. The radiological indexes were below the permissible limits in these mine tailings; therefore, they are safe to use as raw material to produce cement. However, given the heterogeneity of results, it would be advisable to conduct a study for each tailings batch. Incorporating mine tailings into cement production can lead to a decrease in waste release and an improvement in the utilization of natural resources.

The results of the leakage test showed that the system has good tightness, so it can be assumed that the leakage is negligible.

The levels of exhalation found in the tailings to be used as raw material to produce geopolymer cement are very low compared to those reported in other studies. The radon exhalation in the final product should be still lower due to the change in physical properties. At the same time, the gamma radiation could be even more attenuated in the finished material as self-absorption occurs due to the density of the final product.

Mine tailings from different Peruvian mines would be studied with the aim of being used as raw material to produce building materials or for other purposes.

Author Contributions: Conceptualization, R.L.; methodology, R.L., P.P., M.G. and D.P.; formal analysis, R.L., D.P. and L.S.-B.; investigation, R.L. and L.S.-B.; writing—original draft preparation, R.L., J.R. and M.G.; writing—review and editing, R.L., J.R., M.G., L.S.-B., P.P. and D.P.; supervision, D.P., P.P. and L.S.-B.; and funding acquisition, J.R., P.P. and M.G. All authors have read and agreed to the published version of the manuscript.

Funding: This work was supported by the Project CAP 2021-E-0015/ PI 0752 of Pontificia Universidad Católica del Perú and CienciActiva-CONCYTEC 2017.

Institutional Review Board Statement: Not applicable.

Informed Consent Statement: Not applicable.

Data Availability Statement: The data sets generated and/or analyzed during the current study can be obtained from the corresponding author upon reasonable request.

Acknowledgments: This study was carried out as part of the project CAP 2021-E-0015/PI 0752 and the National Council of Science, Technology and Technological Innovation (CONCYTEC) under the PhD scholarship program (236-2015-FONDECYT). The authors thank the GITHUNU-PUCP team for their contributions, especially DM.

Conflicts of Interest: The authors declare no conflict of interest.

References

1. Gayana, B.C.; Chandar, K.R. Sustainable Use of Mine Waste and Tailings with Suitable Admixture as Aggregates in Concrete Pavements—A Review. *Adv. Concr. Constr.* **2018**, *6*, 221–243. [CrossRef]
2. Onuaguluchi, O.; Eren, O. Rheology, strength and durability properties of mortars containing copper tailings as a cement re-placement material. *Eur. J. Environ. Civ. Eng.* **2013**, *17*, 19–31. [CrossRef]
3. Qaidi, S.M.A.; Tayeh, B.A.; Zeyad, A.M.; Azevedo, A.R.G.; Ahmed, H.U.; Emad, W. Recycling of mine tailings for the geopolymers production: A systematic review. *Case Stud. Constr. Mater.* **2022**, *16*, e00933. [CrossRef]
4. Phillip, E.; Choo, T.F.; Khairuddin, N.W.A.; Abdel Rahman, R.O. On the Sustainable Utilization of Geopolymers for Safe Management of Radioactive Waste: A Review. *Sustainability* **2023**, *15*, 1117. [CrossRef]
5. Kamunda, C.; Mathuthu, M.; Madhuku, M. An assessment of radiological hazards from gold mine tailings in the province of Gauteng in South Africa. *Int. J. Environ. Res. Public Health* **2016**, *13*, 138. [CrossRef]
6. Rabuku, A.T.; Malik, A.Q. Natural radioactivity measurement of gold mine tailings in Vatukoula, Fiji Islands. *Renew. Energy Environ. Sustain.* **2020**, *5*, 10. [CrossRef]
7. Ahmari, S.; Zhang, L. Production of eco-friendly bricks from copper mine tailing through geopolimerization. *Constr. Build. Mater.* **2012**, *29*, 323–331. [CrossRef]
8. Nikvar-Hassani, A.; Vashaghian, H.; Hodges, R.; Zhang, L. Production of green bricks from low-reactive copper mine tailings: Chemical and mechanical aspects. *Constr. Build. Mater.* **2022**, *324*, 126695. [CrossRef]
9. Wang, W.; Gan, Y.; Kang, X. Synthesis and characterization of sustainable eco-friendly unburned bricks from slate tailings. *J. Mater. Res. Technol.* **2021**, *14*, 1697–1708. [CrossRef]
10. Wei, Z.; Zhao, J.; Wang, W.; Yang, Y.; Zhuang, S.; Lu, T.; Hou, Z. Utilizing gold mine tailings to produce sintered bricks. *Constr. Build. Mater.* **2021**, *282*, 122655. [CrossRef]
11. Roy, S.; Adhikari, G.R. Use of gold mill tailings in making bricks: A feasibility study. *Waste Manag. Res.* **2007**, *25*, 475–482. [CrossRef] [PubMed]
12. Valdez, J.; Aguilar, J.; Sanchez, L. Diseño e implementación de un proceso alternativo para la fabricación de ladrillos a partir de relaves mineros de Oro. Ingeniare. *Rev. Chil. Ing.* **2020**, *28*, 268–276. [CrossRef]
13. Li, R.; Zhou, Y.; Li, C.; Li, S.; Huang, Z. Recycling of industrial waste iron tailings in porous bricks with low thermal conductivity. *Constr. Build. Mater.* **2019**, *213*, 43–50. [CrossRef]
14. Zhang, N.; Tang, B.; Liu, X. Cementitious activity of iron ore tailing and its utilization in cementitious materials, bricks and concrete. *Constr. Build. Mater.* **2021**, *288*, 123022. [CrossRef]
15. Kuranchie, F.A.; Shukla, S.K.; Habibi, D. Utilisation of iron ore mine tailings for the production of geopolymer bricks. *Int. J. Min. Reclam. Environ.* **2016**, *30*, 92–114. [CrossRef]
16. Thejas, H.K.; Hossiney, N. A short review on environmental impacts and application of iron ore tailings in development of sustainable eco-friendly bricks. *Mater. Today Proc.* **2022**, *61*, 327–331. [CrossRef]
17. Sajedi, F.; Razak, H.A. Hamidreza Nejati, Utilization of copper mine tailings as a partial substitute for cement in concrete construction. *Constr. Build. Mater.* **2022**, *317*, 125921. [CrossRef]
18. Feng, R.; Qi, L. Geopolymerization and its potential application in mine tailings consolidation: A review. *Miner. Process. Extr. Metall. Rev.* **2015**, *36*, 399–409. [CrossRef]
19. Zhao, S.; Fan, J.; Sun, W. Utilization of iron ore tailings as fine aggregate in ultrahigh performance concrete. *Constr. Build. Mater.* **2014**, *50*, 540–548. [CrossRef]
20. Yen, C.-L.; Tseng, D.-H.; Lin, T.-T. Characterization of eco-cement paste produced from waste sludges. *Chemosphere* **2011**, *84*, 220–226. [CrossRef]
21. Paiva, I.; Marques, R.; Santos, M.; Reis, M.; Prudêncio, M.I.; Waerenborgh, J.C.; Pinto, R. Naturally occurring radioactive material and risk assessment of tailings of polymetallic and Ra/U mines from legacy sites. *Chemosphere* **2019**, *223*, 171–179. [CrossRef]
22. Araujo, F.S.; Taborda-Llano, I.; Nunes, E.B.; Santos, R.M. Recycling and reuse of mine tailings: A review of advancements and their implications. *Geosciences* **2022**, *12*, 319. [CrossRef]
23. Xu, D.M.; Zhan, C.L.; Liu, H.X.; Lin, H.Z. A critical review on environmental implications, recycling strategies, and ecological remediation for mine tailings. *Env. Sci. Pollut. Res.* **2019**, *26*, 35657–35669. [CrossRef]
24. Garcia-Troncoso, N.; Baykara, H.; Cornejo, M.H.; Riofrio, A.; Tinoco-Hidalgo, M.; Flores-Rada, J. Comparative mechanical properties of conventional concrete mixture and concrete incorporating mining tailings sands. *Case Stud. Constr. Mater.* **2022**, *16*, e01031. [CrossRef]
25. Kinnunen, P.; Karhu, M.; Yli-Rantala, E.; Kivikytö-Reponen, P.; Mäkinen, J. A review of circular economy strategies for mine tailings. *Clean. Eng. Technol.* **2022**, *8*, 100499. [CrossRef]
26. ICRP. *Lung Cancer Risk from Exposures to Radon Daughters*; ICRP Publication: London, UK, 1987.
27. Ishimori, Y.; Lange, K.; Martin, P.; Mayya, Y.S.; Phaneuf, M. *Measurement and Calculation of Radon Releases from NORM Residues*; U.S. Department of Energy Office of Scientific and Technical Information: Washington, DC, USA, 2013.
28. Nazaroff, W.W.; Nero, A.V. *Radon and Its Decay Products in Indoor Air*; U.S. Department of Energy Office of Scientific and Technical Information: Washington, DC, USA, 1988.
29. Morawska, L.; Phillips, C.R. Dependence of the radon emanation coefficient on radium distribution and internal structure of the material. *Geochim. Cosmochim. Acta* **1993**, *57*, 1783–1797. [CrossRef]

30. Bala, P.; Kumar, V.; Mehra, R. Measurement of radon exhalation rate in various building materials and soil samples. *J. Earth Syst. Sci.* **2017**, *126*, 31. [CrossRef]
31. Kobeissi, M.A.; El-Samad, O.; Rachidi, I. Health assessment of natural radioactivity and radon exhalation rate in granites used as building materials in Lebanon. *Radiat. Prot. Dosim.* **2013**, *153*, 342–351. [CrossRef] [PubMed]
32. Bavarnegin, E.; Fathabadi, N.; Moghaddam, M.V.; Farahani, M.V.; Moradi, M.; Babakhni, A. Radon exhalation rate and natural radionuclide content in building materials of high background areas of Ramsar, Iran. *J. Environ. Radioact.* **2013**, *117*, 36–40. [CrossRef] [PubMed]
33. Turhan, Ş.; Gündüz, L. Determination of specific activity of 226Ra, 232Th and 40K for assessment of radiation hazards from Turkish pumice samples. *J. Environ. Radioact.* **2008**, *99*, 332–342. [CrossRef]
34. Cook, E.M.; DuMont, D. *Process Drying Practice*; McGraw-Hill: New York, NY, USA, 1991.
35. *ASTM C 136—01*; Standard Test Method for Sieve Analysis of Fine and Coarse Aggregates. ASTM International: West Conshohocken, PA, USA, 2020.
36. Vidmar, T.; Vodenik, B. Extended relative method of activity determination. *Appl. Radiat. Isot.* **2010**, *68*, 2421–2424. [CrossRef]
37. Lépy, M.C.; Bé, M.M.; Piton, F. ETNA (Efficiency Transfer for Nuclide activity measurement): Software for efficiency transfer and coincidence summing corrections in gamma-ray spectrometry. *Note Tech. LNHB* **2004**, *1*, 1–48.
38. Gilmore, G. *Practical Gamma-Ray Spectroscopy*; John Wiley & Sons: Hoboken, NJ, USA, 2008.
39. Tuccimei, P.; Castelluccio, M.; Soligo, M.; Moroni, M. Radon exhalation rates of building materials: Experimental, analytical protocol and classification criteria. In *Building Materials*; Nova Science Publishers: Hauppauge, NY, USA, 2009; pp. 259–274.
40. Stajic, J.M.; Nikezic, D. "Measurement of radon exhalation rates from some building materials used in Serbian construction. *J. Radioanal. Nucl. Chem.* **2015**, *303*, 1943–1947. [CrossRef]
41. Kovler, K.; Perevalov, A.; Steiner, V.; Metzger, L.A. Radon exhalation of cementitious materials made with coal fly ash: Part 1—Scientific background and testing of the cement and fly ash emanation. *J. Environ. Radioact.* **2005**, *82*, 321–334. [CrossRef]
42. Lehmann, B.E.; Ihly, B.; Salzmann, S.; Conen, F.; Simon, E. An automatic static chamber for continuous 220Rn and 222Rn flux measurements from soil. *Radiat. Meas.* **2004**, *38*, 43–50. [CrossRef]
43. Tan, Y.; Xiao, D.; Yuan, H.; Tang, Q.; Liu, X. Revision for measuring radon exhalation rate in open loop. *J. Instrum.* **2013**, *8*, T01004. [CrossRef]
44. Gutiérrez-Álvarez, I.; Martín, J.E.; Adame, J.A.; Grossi, C.; Vargas, A.; Bolívar, J.P. Applicability of the closed-circuit ac-cumulation chamber technique to measure radon surface exhalation rate under laboratory conditions. *Radiat. Meas.* **2020**, *133*, 106284. [CrossRef]
45. López-Coto, I.; Mas, J.L.; Bolivar, J.P.; García-Tenorio, R. A short-time method to measure the radon potential of porous materials. *Appl. Radiat. Isot.* **2009**, *67*, 133–138. [CrossRef] [PubMed]
46. Cosma, C.; Cucoş-Dinu, A.; Papp, B.; Begy, R.; Sainz, C. Soil and building material as main sources of indoor radon in Băiţa-Ştei radon prone area (Romania). *J. Environ. Radioact.* **2013**, *116*, 174–179. [CrossRef] [PubMed]
47. European Commission. Radiological Protection Principles Concerning the Natural Radioactivity of Building Materials. In *Radiation Protection 112*; Directorate General Environment, Nuclear Safety and Civil Protection: Luxembourg, 1999.
48. Council Directive 2013/59/Euratom of 5 December 2013 Laying down Basic Safety Standards for Protection against the Dangers Arising from Exposure to Ionising Radiation, and Repealing Directives 89/618/Euratom, 90/641/Euratom, 96/29/Euratom, 97/43/Euratom and 2003/122/Euratom. Off. J. L 2014, 13, 1–73. Available online: https://eur-lex.europa.eu/eli/dir/2013/59/oj (accessed on 15 January 2023).
49. Papadopoulos, A.; Christofides, G.; Koroneos, A.; Papadopoulou, L.; Papastefanou, C.; Stoulos, S. Natural radioactivity and radiation index of the major plutonic bodies in Greece. *J. Environ. Radioact.* **2013**, *124*, 227–238. [CrossRef]
50. Bochicchio, F. Protection from radon exposure at home and at work in the directive 2013/59/Euratom. *Radiat. Prot. Dosim.* **2014**, *160*, 8–13. [CrossRef] [PubMed]
51. Beretka, J.; Mathew, P.J. Natural radioactivity of Australian building materials, industrial wastes and by-products. *Health Phys.* **1985**, *48*, 87–95. [CrossRef]
52. Raghu, Y.; Ravisankar, R.; Chandrasekaran, A.; Vijayagopal, P.; Venkatraman, B. Assessment of natural radioactivity and radiological hazards in building materials used in the Tiruvannamalai District, Tamilnadu, India, using a statistical approach. *J. Taibah Univ. Sci.* **2017**, *11*, 523–533. [CrossRef]
53. Gutiérrez-Álvarez, I.; Guerrero, J.L.; Martín, J.E.; Adame, J.A.; Bolívar, J.P. Influence of the accumulation chamber insertion depth to measure surface radon exhalation rates. *J. Hazard. Mater.* **2020**, *393*, 122344. [CrossRef] [PubMed]
54. Rábago, D.; Quindós, L.; Vargas, A.; Sainz, C.; Radulescu, I.; Ioan, M.R.; Grossi, C. Intercomparison of radon flux monitors at low and at high radium content areas under field conditions. *Int. J. Environ. Res. Public Health* **2022**, *19*, 4213. [CrossRef] [PubMed]
55. UNSCEAR. *Sources and Effects of Ionizing Radiation*; United Nation Scientific Committee on the Effect of Atomic Radiation, United Nation: New York, NY, USA, 2000.

Disclaimer/Publisher's Note: The statements, opinions and data contained in all publications are solely those of the individual author(s) and contributor(s) and not of MDPI and/or the editor(s). MDPI and/or the editor(s) disclaim responsibility for any injury to people or property resulting from any ideas, methods, instructions or products referred to in the content.